

Original Article

Onvansertib inhibits the proliferation and improves the cisplatin-resistance of lung adenocarcinoma via β -catenin/c-Myc signaling pathway

Rong Wang¹, Yihan Hou², Guojun Geng³, Xiaolei Zhu³, Zhilin Wang³, Weifeng Cai³, Juanping Ye², Senxia Zhao², Yanjun Mi², Jie Jiang³

¹Medical College, Guangxi University, Nanning, Guangxi, P.R. China; ²Department of Medical Oncology, Xiamen Key Laboratory of Antitumor Drug Transformation Research, The First Affiliated Hospital of Xiamen University; School of Clinical Medicine, Xiamen University, Xiamen 361003, Fujian Province, P.R. China; ³Department of Thoracic Surgery, Xiamen Key Laboratory of Thoracic Tumor Diagnosis and Treatment, Institute of Lung Cancer, The First Affiliated Hospital of Xiamen University; School of Clinical Medicine, Xiamen University, Xiamen 361003, Fujian Province, P.R. China

Received August 3, 2022; Accepted January 10, 2023; Epub February 15, 2023; Published February 28, 2023

Abstract: Polo-like kinase 1 (PLK1) is a key regulator of cell division, and its abnormal expression is related to the progression and prognosis of cancers. However, the effect of PLK1 inhibitor onvansertib on the growth of lung adenocarcinoma (LUAD) has not been explored. In this study, we performed a series of bioinformatics and experimental analyses to comprehensively investigate the role of PLK1 in LUAD. We used CCK-8 assay and colony formation assay to evaluate the growth inhibitory ability of onvansertib. Furthermore, flow cytometry was applied to exploit the effects of onvansertib on cell cycle, apoptosis, and mitochondrial membrane potential. Moreover, the therapeutic potential of onvansertib was assessed in vivo by using xenograft tumor and patient-derived xenograft (PDX) models. We found that onvansertib significantly induced the apoptosis and inhibited the proliferation and migration of LUAD cells. Mechanistically, onvansertib arrested the cells at G2/M phase and enhanced the levels of reactive oxidative species in LUAD. Accordingly, onvansertib regulated the expression of glycolysis-related genes and improved the cisplatin resistance in LUAD. Notably, the protein levels of β -catenin and c-Myc were affected by onvansertib. Taken together, our findings provide insight into the function of onvansertib and shed light on the potential clinical application of onvansertib for the treatment of patients with LUAD.

Keywords: PLK1, inhibitor, onvansertib, lung adenocarcinoma, bioinformatics

Introduction

Lung cancer is the leading cause of cancer deaths worldwide, which remains a significant challenge to the public health. Non-small cell lung cancer (NSCLC) represents the major lung cancer cases with lung adenocarcinoma (LUAD) as the most common histological subtype [1]. Despite the development of new therapeutic strategies including targeted and immune therapy for the treatment of LUAD, the prognosis of LUAD is still unsatisfactory, particularly the prognosis of patients in the advanced stage. Most patients with LUAD experience recurrence and poor therapeutic response, such that the five-year survival rate was less than 20% [2]. Currently, efforts have been made to identify novel inhibitors targeting the growth of lung

cancer. For example, a potential monoamine oxidase a inhibitor has been reported to suppress the growth and metastasis of paclitaxel-resistant non-small cell lung cancer [3]. However, there is still a lack of effective targeted therapies for this disease. It is an urgent need to identify novel therapeutic targets and develop effective therapeutic drugs for the treatment LUAD.

Mammalian polo-like kinases (PLKs) are a group of conserved serine/threonine protein kinases that play important roles in the process of mitosis including mitotic entry, centrosome maturation, maintenance of the bipolar spindle and mitotic exit [4]. The PLKs family consist of five members (PLK1, PLK2, PLK3, PLK4 and PLK5) and usually exert distinct functions with

little or no overlapping in substrates [5]. Importantly, in humans, PLK1 holds the most pleiotropic and crucial functions during cell cycle. Consistently, the expression of PLK1 is regulated at the G2/M checkpoint by p53. PLK1 can bind to p53 and inhibit its pro-apoptotic function [6, 7]. Previous studies have not only indicated the vital function of PLK1 in normal cell cycle progression [8, 9] but have also revealed the upregulation of PLK1 in pan-cancers as well as the association of PLK1 with the prognosis of various cancers [10-13]. PLK1 controls the proliferation of cancer cells in vitro and in tumor xenograft models [14, 15]. Notably, compared to the effect on normal cells, the growth of tumor cells is more affected by the depletion or decreased expression of PLK1 [16]. Recently, an important study by Deng et al. revealed that higher PLK1/4 expression was significantly related to the prognosis of male patient and patients with TP53 mutant in lung cancer [17], suggesting the potential therapeutic value of PLK1/4. Particularly, considering the specific action of PLK1 on cancer cells without severe effect on the normal cells, it is conceivable that the development of PLK1 inhibitors would be useful in the treatment of patients with LUAD.

Because the specificity of the first generation of PLK1 inhibitors is suboptimal, the second generation of PLK1 inhibitors including onvansertib (also called NMS-1 or NMS-1286937) has been developed with improved specificity and therefore improved safety [18]. Nevertheless, only limited data are available for the effect of onvansertib on tumor growth, and no study on the effect of onvansertib in LUAD was reported. Therefore, in this study, we analyzed the expression of PLK1 by using bioinformatics tools and evaluated the anti-tumor effect of onvansertib in LUAD experimentally in vitro and vivo.

Material and methods

Reagents and cell culture

Onvansertib was purchased from Selleck Chemicals (Shanghai, China). A549 and PC-9 cells were purchased from the Procell (Wuhan, China). Antibodies against Cleaved PARP, Cyclin E1, Cyclin B1, Akt, p-Akt, β -catenin and c-Myc as well as secondary antibodies were purchased from Proteintech, Wuhan, China. All cells were cultured in RPMI-1640 medium

(Thermofisher, Shanghai, China) with 10% FBS and maintained at 37°C with 5% CO₂ in a humidified incubator.

Cell viability assay

A549 and PC-9 cells were seeded into 96-well plates (BIOFIL, Guangzhou, China) at a density of 5,000 cells/well before treated with different concentrations of onvansertib for the indicated time. Cell viability was measured by the Cell Counting Kit-8 assay (APEX BIO, Houston, USA) according to the manufacturer's instructions. Optical density (OD) values at 450 nm were detected with a spectrophotometer. Prism 6.0 (GraphPad, San Diego, USA) was used to process and plot the data.

Cell cycle assay

Cells were collected and washed twice with cold phosphate-buffered saline (PBS), fixed with 70% ice-cold ethanol, and stained with propidium iodide solution (Sangon Biotech, Shanghai, China) at room temperature for 10 minutes in the dark. The cells were then subjected to cell cycle analysis using BD FACSCanto II Flow Cytometer (BD Biosciences, San Jose, USA). Data were processed using FlowJo 10.0 software (Becton Dickinson).

Colony formation assay

A549 and PC-9 cells were plated in a 6-well plate at a density of 500 cells/well, treated with 200 nM onvansertib for 72 h, and then cultured in regular medium for 14 days. Culture medium was replaced every 48-72 h. At the end of the experiments, cells were fixed with methanol and stained with crystal violet (Solarbio, Beijing, China).

Hoechst 33342 staining

Hoechst 33342 (Solarbio, Beijing, China) staining was performed to evaluate the apoptosis of LUAD cell induced by onvansertib treatment. Briefly, cells were cultured in 6-well plates, stained with 10 μ g/ml Hoechst 33342 at room temperature for 20 minutes, washed with PBS, and observed under EVOS M7000 fluorescence microscope (ThermoFisher Scientific, Shanghai, China).

Wound healing assay

The wound healing assay was performed to evaluate the effect of onvansertib on the migra-

Table 1. Primers sequences of real-time PCR

Gene	Forward (5'-3')	Reverse (5'-3')
GLUT1	CTGCTCCTTCATCACAAGTCCA	CCTCCAGTATTTCTGAGTGCC
PDK1	ATCTTACCCCAGCCCATCCAT	GCTCTTGAACGCCTATGTGTCC
LDHA	GCAGCCTTTTCCTTAGAACACC	CCCCAGCCGTGATAATGACC

tion of LUAD cells. Briefly, approximately 10^5 cells were seeded in 6-well plates and treated with onvansertib or vehicle. An artificial wound was then created by wound healing tool (ibidi, Germany), followed by rinsing with PBS to remove the cellular debris. Images of wounded area were acquired at 0h and 24 h using the cell imager (Thermo Scientific, Massachusetts, USA). The wound closure was calculated using ImageJ software version 1.47. Results were presented as the percentage of the respective control groups.

Apoptosis assay

Flow cytometry (FCM) was adopted to evaluate cell apoptosis. Briefly, cells were treated with different concentrations of onvansertib for 48 h, harvested, and stained with Annexin V-FITC Apop Dtec Kits (BD Pharmingen, NJ, USA) according to the manufacturer's instruction. Fluorescence was measured by using BD FACSCanto II Flow Cytometer (BD Biosciences, San Jose, USA). The factions of early apoptotic (Annexin V positive only) and late apoptotic cells (Annexin V and PI positive) were quantified, and the data were analyzed using FlowJo 10.0 software.

Measurement of reactive oxygen species (ROS)

Cells were stained with 10 μ M Dihydroethidium (MCE, USA) at 37°C for 30 minutes and washed with PBS. In each cell, five randomly selected fields were captured under the fluorescent microscope (Thermo Scientific, Massachusetts, USA).

Mitochondrial membrane potential ($\Delta\Psi_m$) assay

LUAD cells were treated with onvansertib, collected, and washed with PBS. Then, the cells were stained with 100 nm fluorescent dye tetramethylrhodamine methyl ester (TMRM) at 37°C for 30 minutes in the dark. As a positive control, a set of cells were stained with 10 uM

carbonyl cyanide 3-chlorophenylhydrazone (CCCP). All cells were analyzed by flow cytometry.

Real-time PCR

Total RNA was extracted from onvansertib-treated cells using TRIzol reagent (Tiangen, Beijing, China) following the manufacturer's protocol and reverse-transcribed into cDNA using a FastKing gDNA Dispelling RT SuperMix (Tiangen, Beijing, China). cDNA was used to quantify gene expression via qPCR using a roche-lightcycler-480 (roche, Switzerland). To determine relative expression, β -actin expression was used as an internal control. The sequences of the primers used for real-time PCR are shown in **Table 1**.

Lentivirus transfection

To establish stable cell lines, lentivirus plasmid was constructed by Maijin Biology (Beijing, China). 24 h before lentivirus transfection, A549 and PC-9 cells were plated into 12-well dishes (1×10^5 cells/well). The original medium substituted for 1 mL of fresh medium containing polybrene and an appropriate virus suspension was added for incubation at 37°C. After 24 h, the medium was replaced with fresh medium without virus. Afterwards, cells were screened with 2 mg/mL puromycin (Solarbio, Beijing, China) to obtain stable cell lines.

Western blot analysis

Briefly, cells were lysed in RIPA buffer (EpiZyme, Shanghai, China) at 4°C for 30 minutes, and the cell lysates were cleared by centrifugation at 12,000 g for 10 minutes. Protein concentrations were determined using BCA method (Absin, Shanghai, China). The protein samples were then separated on SDS-PAGE gels (EpiZyme, Shanghai, China) and transferred onto PVDF membrane (Millipore, Billerica, MA). The membranes were blocked with 5% BSA (Solarbio, Beijing, China) in TBST buffer at room temperature for 1 hour followed by incubation with indicated primary antibodies. After extensive washing, the membranes were incubated with appropriate secondary antibodies, and the signals were developed by the chemiluminescent detection reagents (Advansta, California, USA).

Xenograft tumor model

Four-week-old female nude mice were purchased from Gempharmatech Co., Ltd, Nanjing, China. To establish xenograft tumor, A549 cells (1×10^7 cells per mouse) were subcutaneously inoculated into the flank of mice (n=6). Tumor growth was monitored with a caliper every day, and the tumor volumes were calculated using the formula: volume = (length \times width²)/2. Mice were treated with 60 mg/kg onvansertib by gavage. All animal experiments were approved and conducted in accordance with the guidelines of the Experimental Animal Ethics Committee of Xiamen University.

Patient-derived xenograft (PDX) models

Athymic nu/nu nude mice (Gempharmatech Co., Ltd, Nanjing, China), 4-6 weeks old, were used for this study. Fresh tumor fragments were transplanted subcutaneously (s.c.) into the left flank of mice. Tumor growth was measured in 2 dimensions with a caliper. Tumor volumes (TV) were determined by the formula: TV = (length \times width²)/2. Tumors were routinely passaged at TV = 1 cm³. Mice were treated with 60 mg/kg onvansertib. Animal experiments were conducted in accordance with the guidelines of the Experimental Animal Ethics Committee of Xiamen University.

Statistical analysis

Experiments were repeated at least three times, and the results were displayed as the means \pm standard deviations. Student's t-test or one-way ANOVA was utilized to determine the statistical differences between different groups. The *P* value less than 0.05 was considered statistically significant.

Results

Upregulation of PLK1 in LAUD and its correlation with the prognosis of LUAD

In order to assess the expression of PLK1 and its correlation with prognosis in LUAD patients, we performed bioinformatics analysis using the data from TCGA database and K-M plot database. Our results indicated that the expression of PLK1 was upregulated in multiple cancer types (**Figure 1A**), which was further confirmed experimentally. We found that the expression of

PLK1 was higher in LUAD tumor tissues than in normal tissues (**Figure 1B, 1C**). Moreover, as shown in **Figure 1D**, the patients with high PLK1 expression had worse prognosis than those with low PLK1 expression ($P < 0.05$). Multi-factor regression analysis also suggested that the expression of PLK1 was an independent prognostic factor of LUAD (**Figure 1E**).

Onvansertib inhibits the growth of LUAD

Given the above data that PLK1 was upregulated in LUAD, we explored the effect of PLK1 inhibitor onvansertib in the tumorigenesis of LUAD. Two LUAD cancer cell lines (A549 and PC-9) were treated with different concentrations of onvansertib, while DMSO treatment was used as negative control. The cell growth was assayed, and the data indicated that onvansertib obviously inhibited the growth of A549 and PC-9 cells, with the IC₅₀ in the nanomolar range (**Figure 2A, 2B**). Morphological changes of LUAD cells were also observed after onvansertib treatment (**Figure 2C, 2D**). Furthermore, as shown in **Figure 2E, 2F**, the colony formation of LUAD cells was markedly inhibited by onvansertib.

Onvansertib causes the G2/M arrest of LUAD cells

To explore whether onvansertib influences the cell cycle progression of LUAD, we treated LUAD cells with different concentrations of onvansertib for 48 h. Interestingly, onvansertib increased the proportion of cells at G2/M phase in both A549 and PC-9 cells (**Figure 3A-D**). Consistently, western blot analysis demonstrated that onvansertib treatment resulted in the accumulation of Cyclin B1 and the decrease of Cyclin E1, an indicator of altered cell cycle progression (**Figure 3E, 3F**).

Onvansertib induces apoptosis in LUAD cells

We also investigated the effect of onvansertib on the apoptosis of A549 and PC-9 cells by using Annexin V-staining in FCM analysis. We observed increasing percentage of apoptotic cells along with the increasing concentrations of onvansertib (**Figure 4A-F**), which could be rescued by the ROS scavenger N-acetyl-L-cysteine (NAC). We further used Hoechst 33258 staining to confirm the apoptosis-induc-

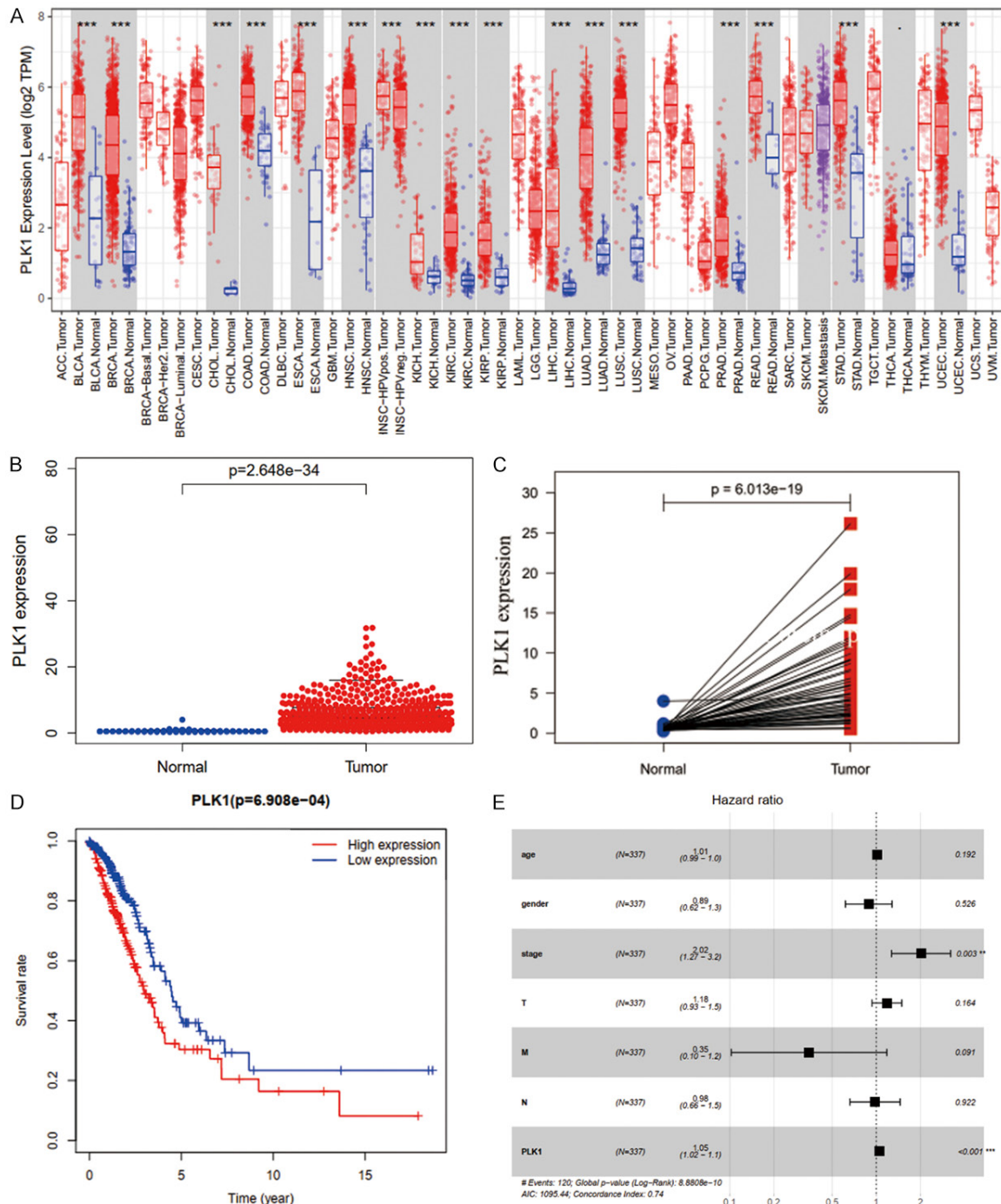


Figure 1. The expression of PLK1 and its association with the prognosis of LUAD. A. PLK1 expression in the normal and tumor samples of pan-cancers. B and C. PLK1 expression in normal and tumor samples of LUAD. D. Correlation between PLK1 expression and the prognosis of LUAD. E. Multi-factor regression analysis of LUAD.

ing effect of onvansertib. As expected, onvansertib enhanced A549 and PC-9 cell death (Figure 4G, 4H) and the elevated expression of cleaved PARP, as determined by western blotting (Figure 4I, 4J).

Onvansertib inhibits the migration of LUAD cells

The wound healing assay was performed to determine the effect of onvansertib on cell

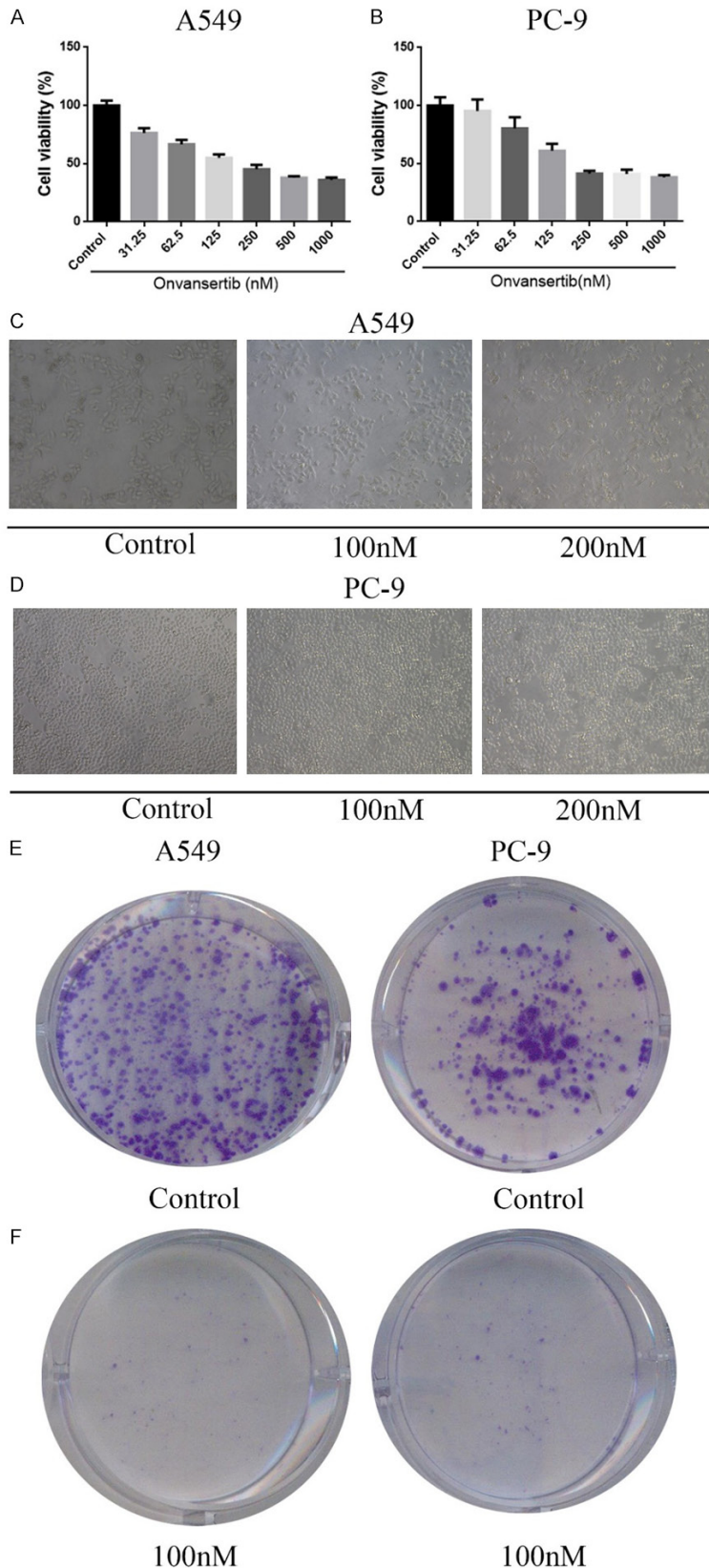


Figure 2. Onvansertib inhibits the growth of LUAD cells. A and B. The growth curves of A549 cells and PC-9 cells treated with different concentrations of onvansertib. C and D. Morphological changes in cells treated with onvan-

sertib. E and F. Colony formation of A549 cells and PC-9 cells in the presence of onvansertib.

migration. In untreated cells, complete wound closure was achieved within 24 h; however, onvansertib significantly attenuated the wound closure, an indicator of suppressed cell migration, in both A549 (Figure 5A, 5B) and PC-9 (Figure 5C, 5D) cells.

Onvansertib affects mitochondrial function in LUAD cells

The mitochondrion is a common target for anticancer drugs to induce apoptosis, and the loss of mitochondrial membrane potential represents the early step during the apoptotic progression. Furthermore, ROS plays a vital role in the anticancer drug resistance and cancer cell death. In this study, we used Dihydroethidium to measure the ROS levels. As shown in Figure 6A, 6B, onvansertib increased the ROS accumulation in A549 and PC-9 cells, which could be completely reversed by NAC. We further used the TMRM staining to determine the levels of mitochondrial membrane potential (MMP) by flow cytometry. Consistently, the MMP in both A549 and PC-9 cells was remarkably reduced by onvansertib treatment (Figure 6C, 6D).

β -catenin/c-Myc signaling pathway is involved in the effect of onvansertib

To understand the mechanisms involved in the effects of onvansertib, we first performed the bioinformatics analysis based on the differential expression of PLK1 and c-Myc in LUAD samples in the

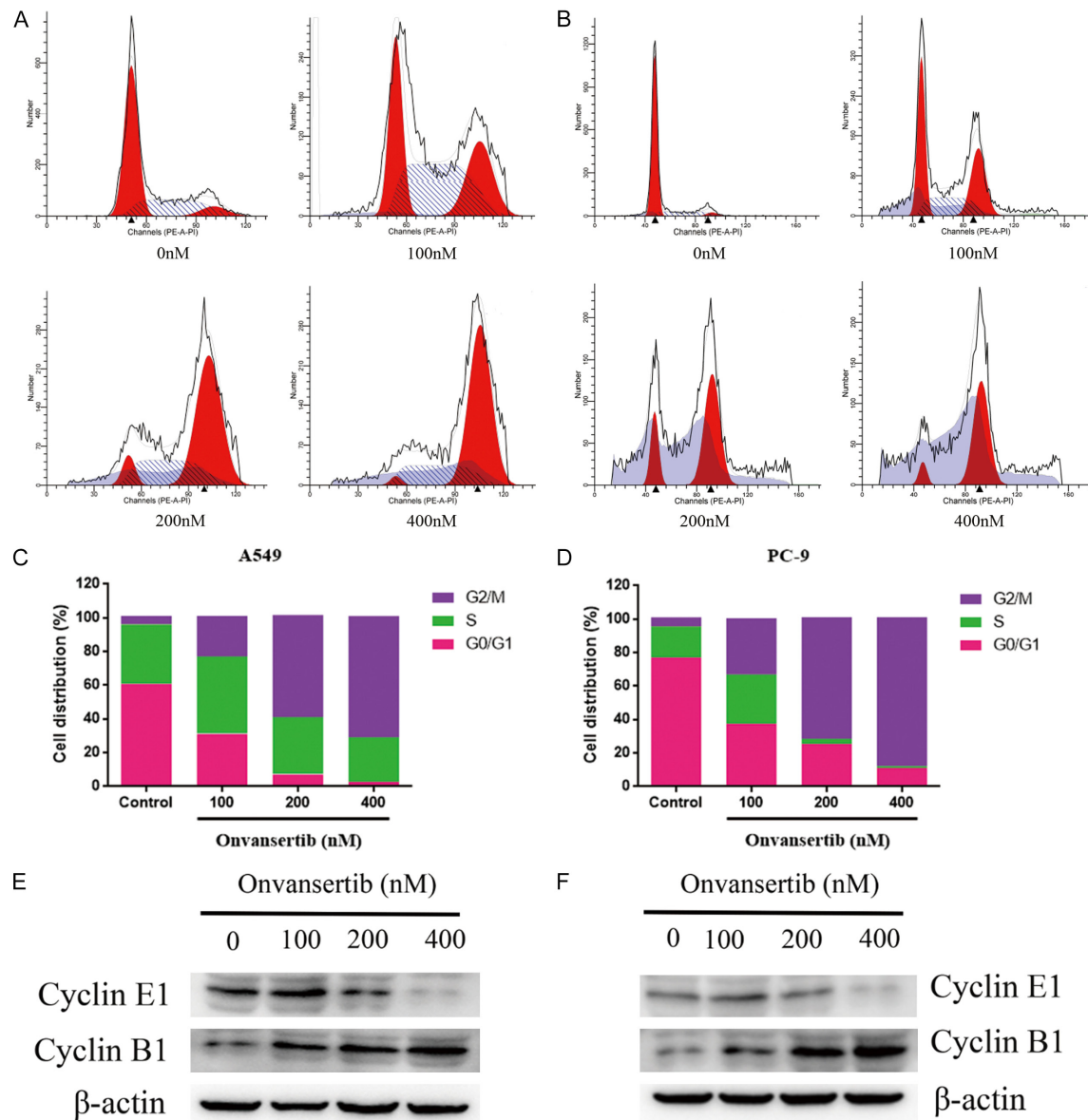
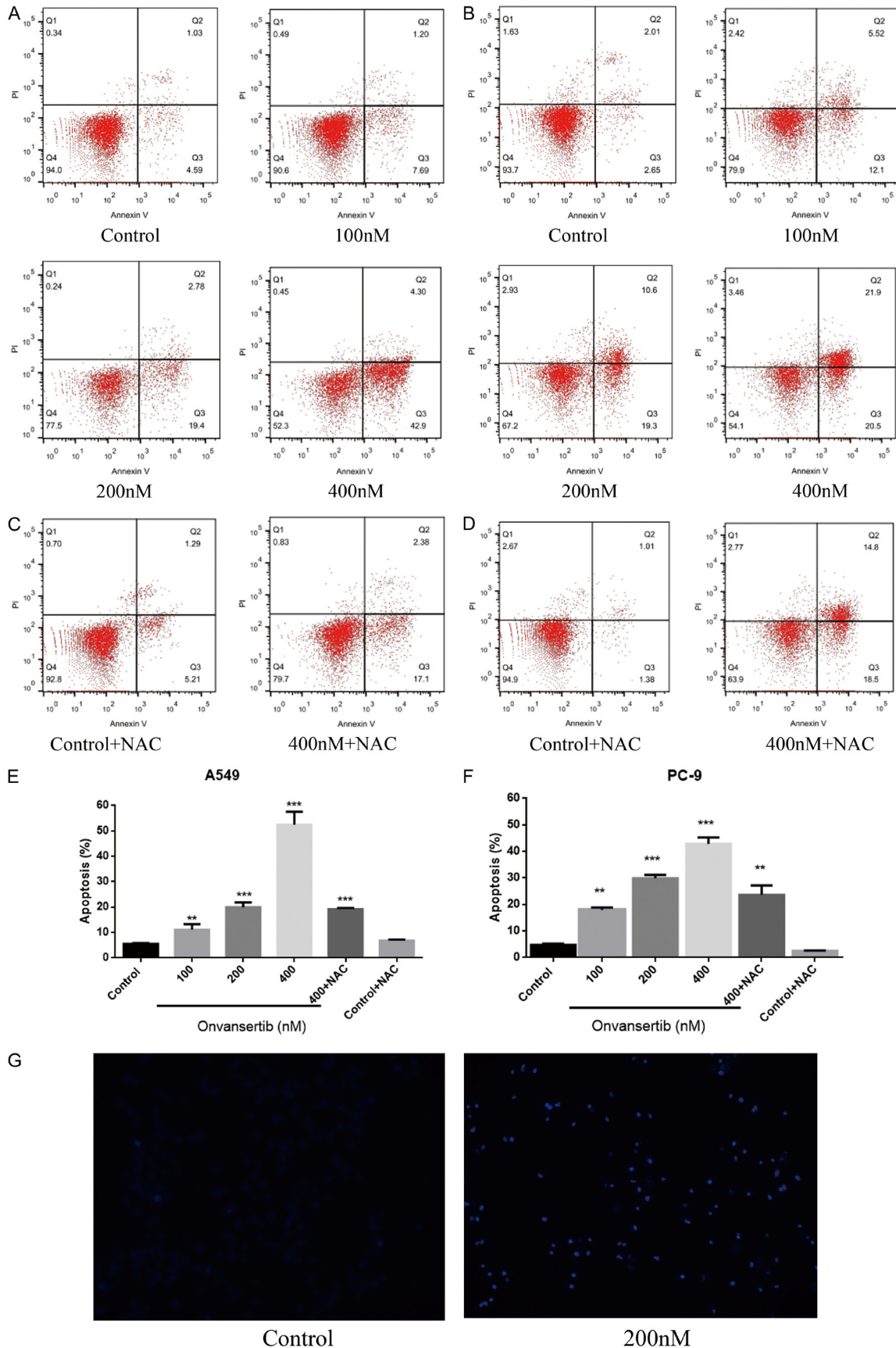


Figure 3. Onvansertib induces cell cycle arrest at G2/M phase in LUAD cells. A and C. The cell cycle distribution of A549 cells was measured by FCM with PI staining. B and D. The cell cycle distribution of PC-9 cells. E and F. The expression of Cyclin B1 and Cyclin E1 proteins was examined by western blotting.

TCGA database. Interestingly, we found that the β -catenin signaling pathway was enriched in LUAD, and the expression of PLK1 was correlated with the expression of c-Myc, a downstream target gene of PLK1 (Figure 7A, 7B). Hence, we examined the expression of β -catenin and c-Myc in A549 and PC-9 cells upon onvansertib treatment and found dramatic changes induced by onvansertib (Figure 7C, 7D). This effect was partially reversed by over-expressed c-Myc (Supplementary Figure 1A-C). Moreover, we also found that onvansertib can

downregulated the protein expressions of p-Akt (Supplementary Figure 2A, 2B). Next, given the regulatory role of c-Myc in glycolysis and cisplatin resistance, we also assessed the expression of glycolysis-associated genes and revealed that the mRNA levels of GLUT1, PDK1 and LDHA were decreased by onvansertib treatment (Figure 7E, 7F). Furthermore, when testing the effect of the combination of onvansertib and cisplatin, we found a strong synergistic effect between them in cisplatin-resistance A549 cells (Figure 7G). To quantitatively evalu-

Onvansertib and LUAD



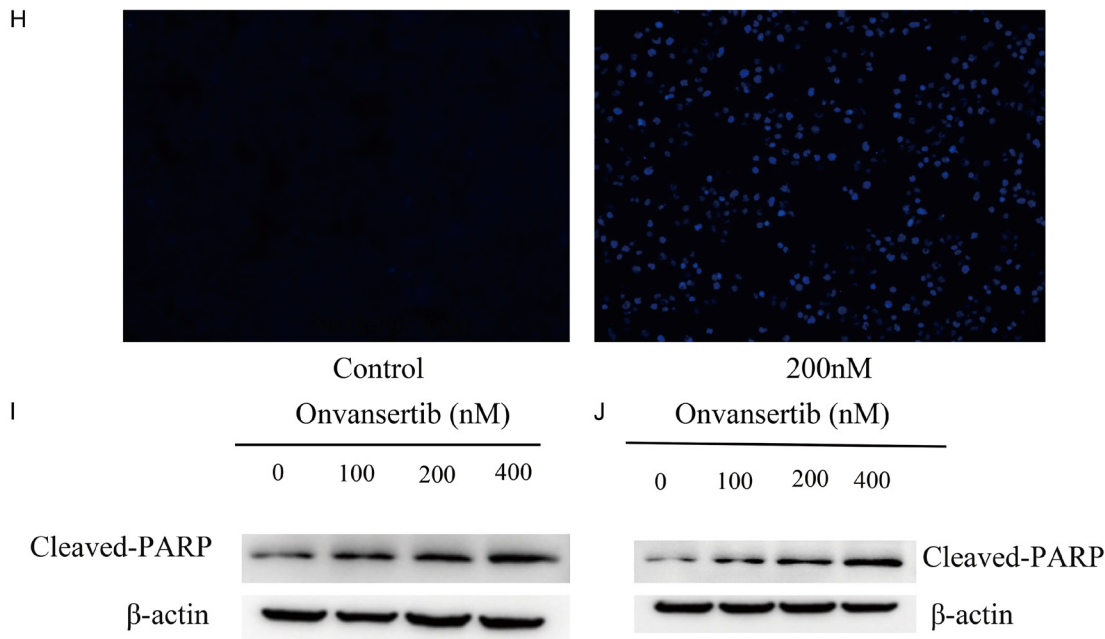


Figure 4. Onvansertib enhances apoptosis in LUAD cells. (A-D) The apoptosis of A549 cells (A, C) and PC-9 (B, D) cells was measured by FCM using Annexin V/PI staining. (E and F) The proportion of apoptosis was calculated in all cells. (G and H) Hoechst 33342 staining of onvansertib-treated A549 cells and PC-9 cells. (I and J) The expression of cleaved PARP was detected by western blotting.

ate the interaction between onvansertib and cisplatin, we adopted the method by Zheng-jun Jing, in which a Q value was calculated to represent the relationship of the two parties: $Q \leq 0.85$ represents an antagonistic effect; $0.85 \leq Q < 1.15$ represents an additive effect, while $Q > 1.15$ represents a synergy effect. The Q value of onvansertib and cisplatin was >1.15 , indicating the synergistic effect of onvansertib and cisplatin when used in combination (Figure 7H).

Onvansertib inhibits tumor growth in xenograft model and PDX models

Having observed the growth inhibitory effect of onvansertib in vitro, we further investigated the effect of onvansertib in vivo by using A549 cells-derived xenograft tumor model. When the mice were fed with a dose of onvansertib (60 mg/kg), we observed a decreased tumor growth (Figure 8A, 8B). The tumor weight was significantly reduced by onvansertib treatment (Figure 8C), whereas the bodyweight of mice was not significantly affected (Figure 8D). Moreover, vivo experimental results of PDX models also showed that onvansertib inhibits the tumor growth (Figure 8E, 8F). The tumor weight was significantly reduced by onvansertib

treatment (Figure 8G). Onvansertib was safe and well tolerated as demonstrated by the lack of significant body weight loss (Figure 8H).

Discussion

Lung cancer is the leading cause of cancer deaths worldwide, among which LUAD exhibits rapid tumor growth and the development of metastasis, thereby leading to cancer death [19]. Although new treatment options are emerging during the last decade, the overall survival (OS) in LUAD is still unsatisfactory. Hence, it is urgent to develop more treatment strategies for LUAD.

In this study, we used the bioinformatics tools to analyze the data from publicly available database and found an upregulation of PLK1 in LUAD. In addition, we found that LUAD patients with higher expression of PLK1 have a lower survival rate, suggesting that PLK1 might be a potential therapeutic target for LUAD. To test this, we first investigated the effect of onvansertib, a PLK1 inhibitor, on the growth of LUAD cells in vitro, and our results indicated that onvansertib could significantly suppress the growth and migration of LUAD cells. Mechanistically, onvansertib arrested cells at G2/M

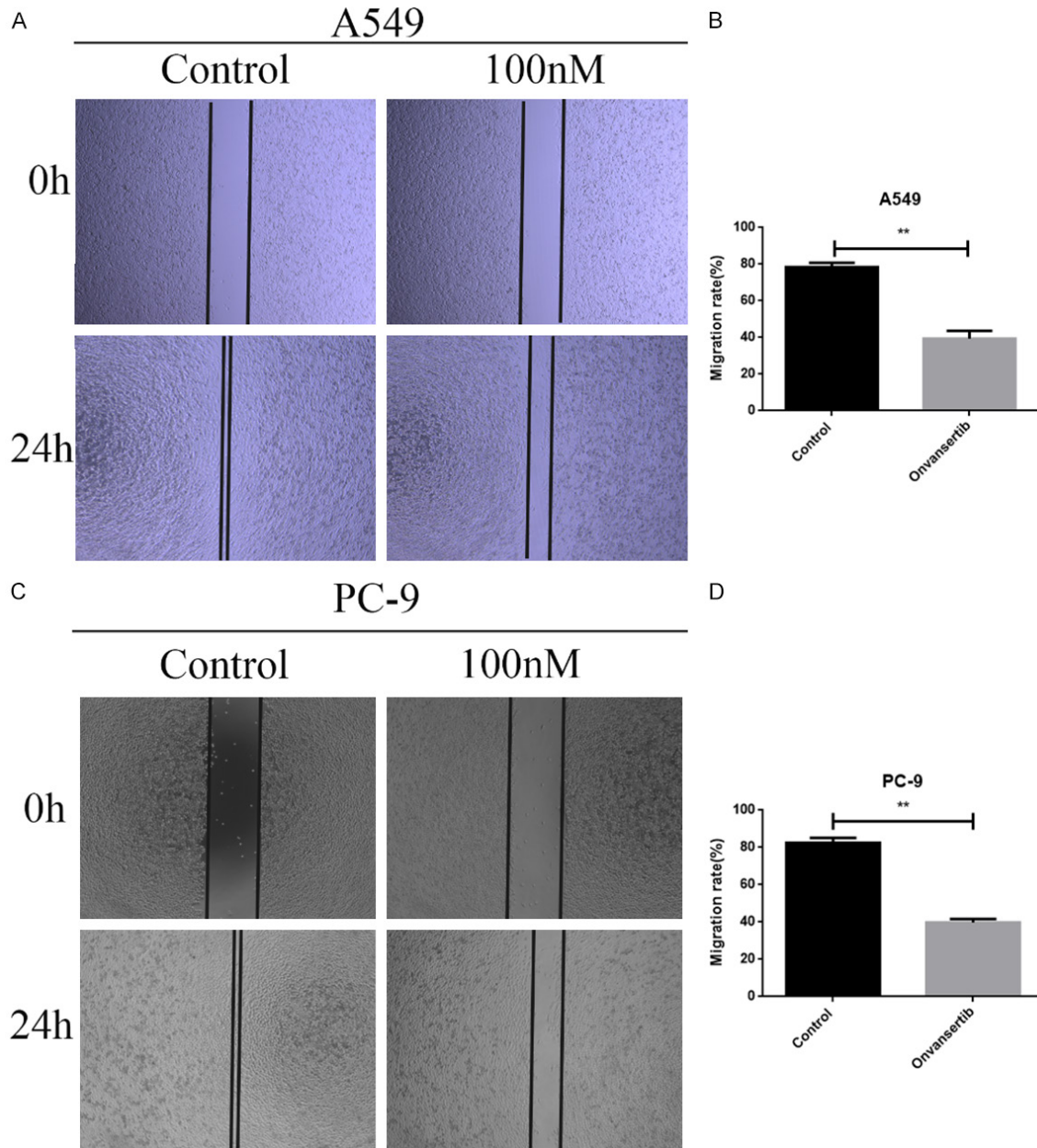


Figure 5. Onvansertib inhibits the migration of LUAD cells. A and B. Wound healing assay of A549 cells. The wound closure was determined. C and D. Wound healing assay of PC-9 cells. The wound closure was determined.

phase by increasing cyclin E1 level, while inhibiting cyclin B1 level. Furthermore, onvansertib could raise the level of ROS in a dose-dependent manner. Since ROS scavenger NAC could partially decrease the level of ROS and apoptosis, we believed that the increased ROS levels mediate the apoptosis of LUAD cells induced by onvansertib treatment. It has been well known that ROS is produced by two sources: oxidative protein folding machinery of the endoplasmic reticulum (ER) and mitochondria.

During the depletion of mitochondrial transmembrane potential ($\Delta\Psi_m$), original ROS is made in the mitochondria. In line with our ROS data, mitochondrial transmembrane potential was also decreased by onvansertib. Furthermore, in consistent with the notion that the attenuation of $\Delta\Psi_m$ can activate caspase 9 and the subsequent cleavage of caspase 3, we also found that the expression of apoptosis-associated proteins was regulated accordingly by onvansertib. At molecular level, we revealed

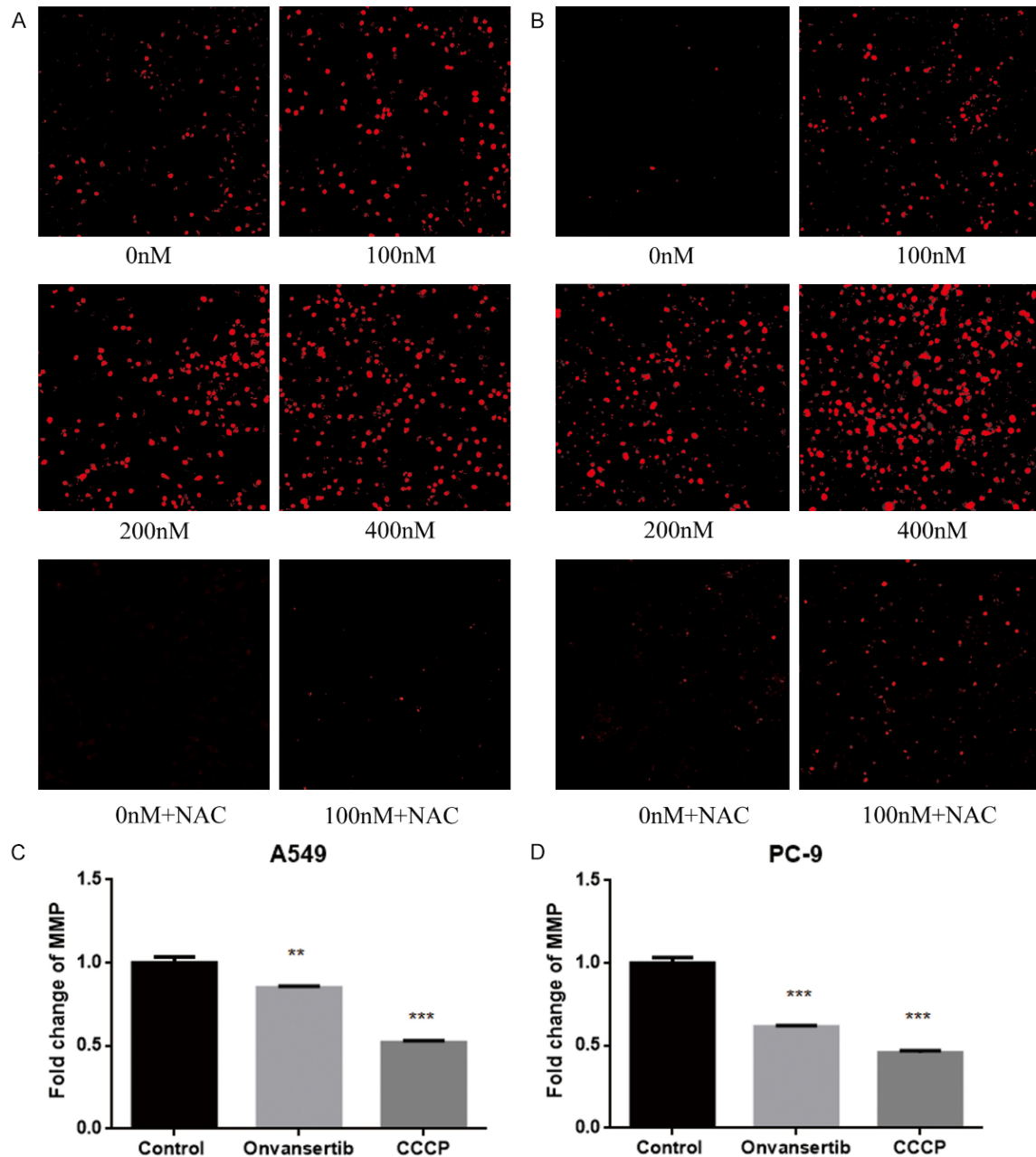


Figure 6. Onvansertib increases the level of ROS and decreases the level of mitochondrial membrane potential in LUAD cells. A and B. The ROS levels in cells treated with onvansertib or treated with NAC and DHE. C and D. The mitochondrial membrane potential was measured by FCM using TMRM staining.

that β -catenin/c-Myc signaling was affected by onvansertib. More importantly, *vivo* xenograft tumor model and PDX models supported our findings that onvansertib inhibited the growth of LUAD cells. Together, these results illustrated the potential application of onvansertib in the treatment of LUAD. However, the evaluation of future clinical trials for onvansertib to identify appropriate patients for treatment.

Onvansertib is a novel PLK1-specific inhibitor which has been evaluated in several solid and hematologic tumors [20]. In preclinical studies, onvansertib has been shown to markedly inhibit the growth of HT29 human colon adenocarcinoma xenografts when combined with irinotecan and to increase the survival of animals in a disseminated model of acute myelogenous leukemia when combined with cytarabine [21]. In

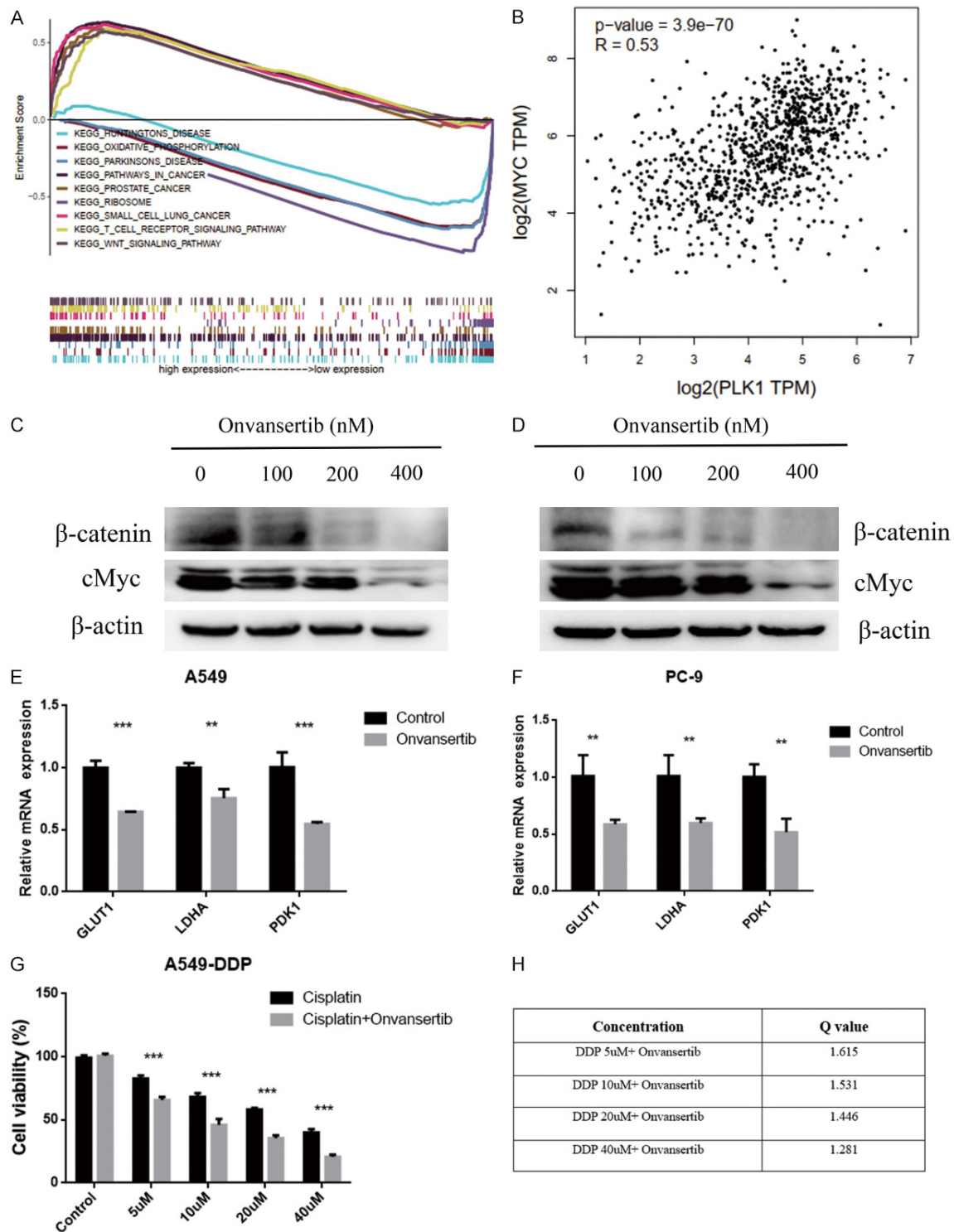


Figure 7. Onvansertib inhibits the expression of β -catenin and c-Myc in LUAD cells. **A.** Enrichment analysis of differentially expressed genes. **B.** Correlation between the expression of c-Myc and PLK1. **C** and **D.** The expression levels of β -catenin and c-Myc in onvansertib-treated A549 and PC-9 cells. **E** and **F.** The mRNA expression levels of GLUT1, PDK1 and LDHA in onvansertib-treated cells. **G.** The synergistic effect from the combination of onvansertib and cisplatin in cisplatin-resistance A549 cells. **H.** Q value calculation of the combination of onvansertib and cisplatin.

additional, a study by Alessia et al. reported that onvansertib prolonged the median survival

time (MST) in CD56 (+) acute monoblastic leukemia. Furthermore, onvansertib mediates

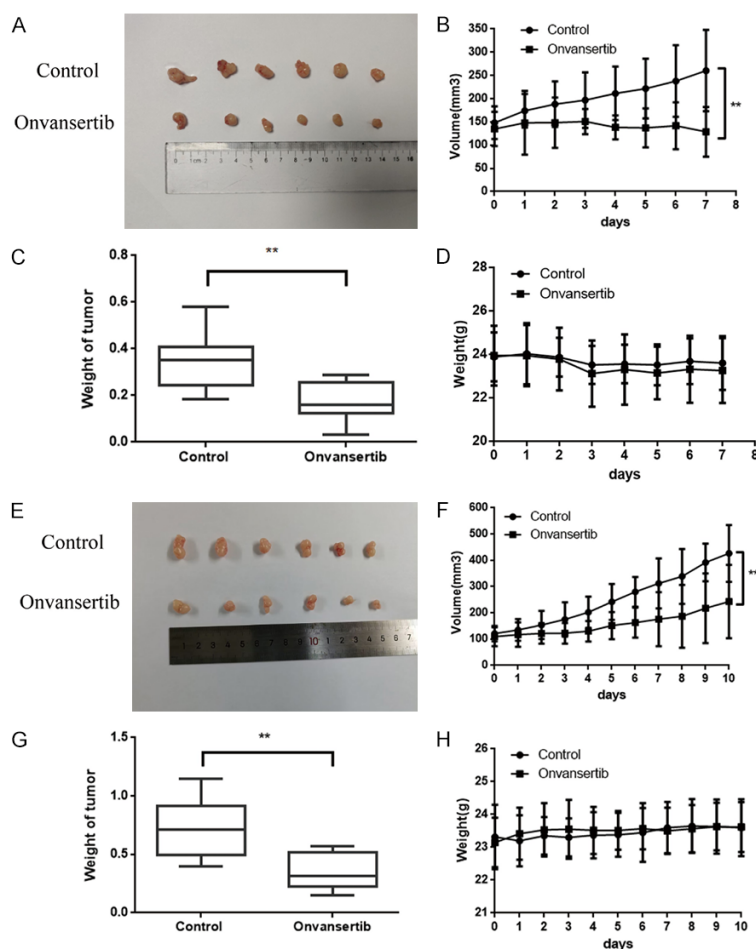


Figure 8. Onvansertib inhibits the growth of LUAD cell-derived xenograft tumor and PDX models. Mice were treated with onvansertib in LUAD cell-derived xenograft tumor and PDX models with onvansertib (60 mg/kg) by gavage. A and E. Tumor images. B and F. Tumor volumes. C and G. Tumor weights. D and H. Carcass weights.

specific biomarker modulation in extramedullary tissues [22]. Moreover, onvansertib is highly effective in drug-sensitive and drug-resistant cell lines. In these cells, the combination of onvansertib with Doxorubicin can reverse the Doxorubicin-resistance by negatively interfering with ABCB1 transport activity. Similar to previous reports that onvansertib inhibits the clonogenic and migration ability of osteosarcoma cells [23], we also found that onvansertib can inhibit the growth and migration of LUAD. PLK1 has also been implicated in the metastatic dissemination and malignancy of other neoplasms. Regarding the functional mechanism of PLK1, PLK1 regulation of Wnt/ β -catenin signal pathway has been suggested. For example, PLK1 can regulate hepatic stellate cell activation and liver fibrosis via the Wnt/ β -catenin sig-

naling pathway [24]. In this study, we were the first to report that PLK1 inhibitor onvansertib could influence β -catenin/c-Myc signaling pathway. It is well known that the expression of c-Myc is tightly regulated in normal cells, as the abnormal expression of c-Myc has been detected in most human cancers. Importantly, c-Myc is a critical regulator of glycolysis-related genes. The PLK1 inhibitor BI25-36 substantially downregulated the mRNA levels of GLUT1, LDHA and PDK1 in U-2 OS cells [25]. Likewise, we also found that onvansertib could downregulate their mRNA levels. In addition, onvansertib has been implicated in chemo-sensitivity. Wu et al. [15] showed that onvansertib could enhance the chemo-sensitivity of cisplatin by inducing pyroptosis in esophageal squamous cell carcinoma. Similarly, in head and neck squamous cell carcinoma, onvansertib combined with cisplatin and/or radiotherapy resulted in a synergic induction of tumor cell death [26]. We also found a synergistic effect between onvansertib and cis-

platin in cisplatin-resistance LUAD cells, which warrants further investigation.

In conclusion, our study provided evidence to support the notion that onvansertib is a potent inhibitor targeting the growth and cisplatin resistance of LUAD. It significantly suppresses the proliferation and migration as well as enhances the apoptosis of LUAD through the β -catenin/c-Myc signaling pathway. Thus, onvansertib will be used in the clinical treatment of patients with LUAD.

Acknowledgements

This study was supported by The National Nature Science Foundation of China (No. 81871877; 31900542), The Natural Science

Foundation of Fujian Province (No. 2016J016-36, 2017J01363, 2018J01374), The Research Fund of Fujian Province Health and Family Planning Commission (No. 2017-ZQN-86, 2018-CXB-23), and the Clinical Research Fund of Xiamen (3502Z20189007).

Disclosure of conflict of interest

None.

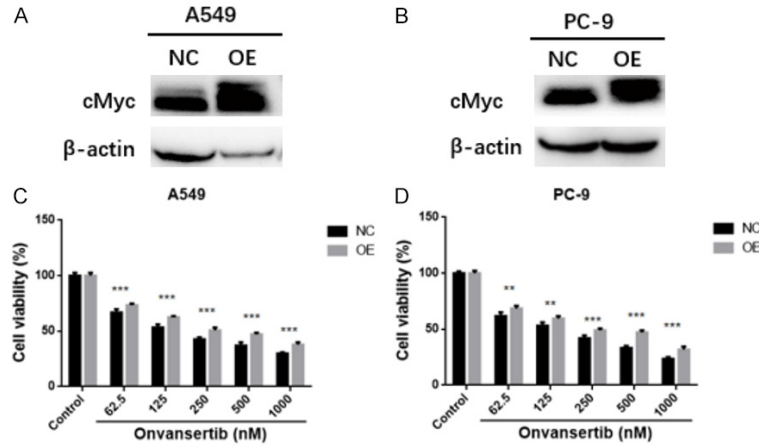
Address correspondence to: Yanjun Mi, Department of Medical Oncology, Xiamen Key Laboratory of Antitumor Drug Transformation Research, The First Affiliated Hospital of Xiamen University; School of Clinical Medicine, Xiamen University, Xiamen 361-003, Fujian Province, P.R. China. E-mail: Miyj77@xmu.edu.cn; Jie Jiang, Department of Thoracic Surgery, Xiamen Key Laboratory of Thoracic Tumor Diagnosis and Treatment, Institute of Lung Cancer, The First Affiliated Hospital of Xiamen University; School of Clinical Medicine, Xiamen University, Xiamen 361003, Fujian Province, P.R. China. E-mail: jiejiangfy@163.com

References

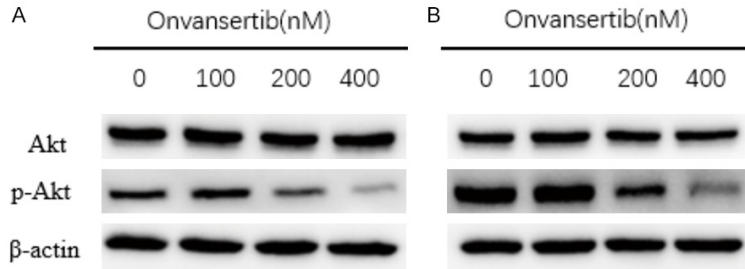
- [1] Herbst RS, Heymach JV and Lippman SM. Lung cancer. *N Engl J Med* 2008; 359: 1367-1380.
- [2] Miller KD, Nogueira L, Mariotto AB, Rowland JH, Yabroff KR, Alfano CM, Jemal A, Kramer JL and Siegel RL. Cancer treatment and survivorship statistics, 2019. *CA Cancer J Clin* 2019; 69: 363-385.
- [3] Liu M, Cui L, Li X, Xia C, Li Y, Wang R, Ren F, Liu H and Chen J. PD-0332991 combined with cisplatin inhibits nonsmall cell lung cancer and reversal of cisplatin resistance. *Thorac Cancer* 2021; 12: 924-931.
- [4] Brandt JN, Hussey KA and Kim Y. Spatial and temporal control of targeting polo-like kinase during meiotic prophase. *J Cell Biol* 2020; 219: e202006094.
- [5] Archambault V, Lépine G and Kachaner D. Understanding the polo kinase machine. *Oncogene* 2015; 34: 4799-4807.
- [6] Ando K, Ozaki T, Yamamoto H, Furuya K, Hosoda M, Hayashi S, Fukuzawa M and Nakagawara A. Polo-like kinase 1 (Plk1) inhibits p53 function by physical interaction and phosphorylation. *J Biol Chem* 2004; 279: 25549-25561.
- [7] Takeshita T, Asaoka M, Katsuta E, Photiadis SJ, Narayanan S, Yan L and Takabe K. High expression of polo-like kinase 1 is associated with TP53 inactivation, DNA repair deficiency, and worse prognosis in ER positive Her2 negative breast cancer. *Am J Transl Res* 2019; 11: 6507-6521.
- [8] Shakeel I, Basheer N, Hasan GM, Afzal M and Hassan MI. Polo-like kinase 1 as an emerging drug target: structure, function and therapeutic implications. *J Drug Target* 2021; 29: 168-184.
- [9] Takeda Y, Yamazaki K, Hashimoto K, Watanabe K, Chinen T and Kitagawa D. The centriole protein CEP76 negatively regulates PLK1 activity in the cytoplasm for proper mitotic progression. *J Cell Sci* 2020; 133: jcs241281.
- [10] de Cárcer G, Venkateswaran SV, Salgueiro L, El Bakkali A, Somogyi K, Rowald K, Montañés P, Sanclemente M, Escobar B, de Martino A, McGranahan N, Malumbres M and Sotillo R. Plk1 overexpression induces chromosomal instability and suppresses tumor development. *Nat Commun* 2018; 9: 3012.
- [11] Gheghiani L, Wang L, Zhang Y, Moore XTR, Zhang J, Smith SC, Tian Y, Wang L, Turner K, Jackson-Cook CK, Mukhopadhyay ND and Fu Z. PLK1 induces chromosomal instability and overrides cell-cycle checkpoints to drive tumorigenesis. *Cancer Res* 2021; 81: 1293-1307.
- [12] Li K, Ma H, Zheng X, Hu Y, Wang Y, Zhang K, Chen J, Qi Y, Jiang J, Pang L, Tao L, Gu W, Li F and Zou H. Overexpression of polo-like kinase1 (PLK1) in chondrosarcoma and its implications for cancer progression. *Int J Clin Exp Pathol* 2018; 11: 1707-1711.
- [13] Li Z, Liu J, Li J, Kong Y, Sandusky G, Rao X, Liu Y, Wan J and Liu X. Polo-like kinase 1 (Plk1) overexpression enhances ionizing radiation-induced cancer formation in mice. *J Biol Chem* 2017; 292: 17461-17472.
- [14] Dang SC, Fan YY, Cui L, Chen JX, Qu JG and Gu M. PLK1 as a potential prognostic marker of gastric cancer through MEK-ERK pathway on PDX models. *Onco Targets Ther* 2018; 11: 6239-6247.
- [15] Wu M, Wang Y, Yang D, Gong Y, Rao F, Liu R, Danna Y, Li J, Fan J, Chen J, Zhang W and Zhan Q. A PLK1 kinase inhibitor enhances the chemosensitivity of cisplatin by inducing pyroptosis in oesophageal squamous cell carcinoma. *EBioMedicine* 2019; 41: 244-255.
- [16] Zhang X, Schuhmachers P, Mourão A, Giansanti P, Murer A, Thumann S, Kuklik-Roos C, Beer S, Hauck SM, Hammerschmidt W, Küppers R, Kuster B, Raab M, Strebhardt K, Sattler M, Münz C and Kempkes B. PLK1-dependent phosphorylation restrains EBNA2 activity and lymphomagenesis in EBV-infected mice. *EMBO Rep* 2021; 22: e53007.
- [17] Elsayed I and Wang X. PLK1 inhibition in cancer therapy: potentials and challenges. *Future Med Chem* 2019; 11: 1383-1386.

- [18] Beria I, Bossi RT, Brasca MG, Caruso M, Ceccarelli W, Fachin G, Fasolini M, Forte B, Fiorentini F, Pesenti E, Pezzetta D, Posteri H, Scolari A, Re Depaolini S and Valsasina B. NMS-P937, a 4, 5-dihydro-1H-pyrazolo [4, 3 h] quinazoline derivative as potent and selective polo-like kinase 1 inhibitor. *Bioorg Med Chem Lett* 2011; 21: 2969-2974.
- [19] Shi J, Lv X, Li W, Ming Z, Zeng L, Yuan J, Chen Y, Liu B and Yang S. Overexpression of BCCIP predicts an unfavorable prognosis and promotes the proliferation and migration of lung adenocarcinoma. *Thorac Cancer* 2021; 12: 2324-2338.
- [20] Hartsink-Segers SA, Exalto C, Allen M, Williamson D, Clifford SC, Horstmann M, Caron HN, Pieters R and Den Boer ML. Inhibiting polo-like kinase 1 causes growth reduction and apoptosis in pediatric acute lymphoblastic leukemia cells. *Haematologica* 2013; 98: 1539-1546.
- [21] Valsasina B, Beria I, Alli C, Alzani R, Avanzi N, Ballinari D, Cappella P, Caruso M, Casolaro A, Ciavolella A, Cucchi U, De Ponti A, Felder E, Fiorentini F, Galvani A, Gianellini LM, Giorgini ML, Isacchi A, Lansen J, Pesenti E, Rizzi S, Rocchetti M, Sola F and Moll J. NMS-P937, an orally available, specific small-molecule polo-like kinase 1 inhibitor with antitumor activity in solid and hematologic malignancies. *Mol Cancer Ther* 2012; 11: 1006-1016.
- [22] Casolaro A, Golay J, Albanese C, Ceruti R, Patton V, Cribioli S, Pezzoni A, Losa M, Texido G, Giussani U, Marchesi F, Amboldi N, Valsasina B, Bungaro S, Cazzaniga G, Rambaldi A, Introna M, Pesenti E and Alzani R. The polo-like kinase 1 (PLK1) inhibitor NMS-P937 is effective in a new model of disseminated primary CD56⁺ acute monoblastic leukaemia. *PLoS One* 2013; 8: e58424.
- [23] Sero V, Tavanti E, Vella S, Hattinger CM, Fanelli M, Michelacci F, Versteeg R, Valsasina B, Gudeman B, Picci P and Serra M. Targeting polo-like kinase 1 by NMS-P937 in osteosarcoma cell lines inhibits tumor cell growth and partially overcomes drug resistance. *Invest New Drugs* 2014; 32: 1167-1180.
- [24] Chen Y, Chen X, Ji YR, Zhu S, Bu FT, Du XS, Meng XM, Huang C and Li J. PLK1 regulates hepatic stellate cell activation and liver fibrosis through Wnt/ β -catenin signalling pathway. *J Cell Mol Med* 2020; 24: 7405-7416.
- [25] Mo H, He J, Yuan Z, Wu Z, Liu B, Lin X and Guan J. PLK1 contributes to autophagy by regulating MYC stabilization in osteosarcoma cells. *Oncotargets Ther* 2019; 12: 7527-7536.
- [26] Hagege A, Ambrosetti D, Boyer J, Bozec A, Doyen J, Chamorey E, He X, Bourget I, Rousset J, Saada E, Rastoin O, Parola J, Luciano F, Cao Y, Pagès G and Dufies M. The Polo-like kinase 1 inhibitor onvansertib represents a relevant treatment for head and neck squamous cell carcinoma resistant to cisplatin and radiotherapy. *Theranostics* 2021; 11: 9571-9586.

Onvansertib and LUAD



Supplementary Figure 1. C-Myc activation rescued onvansertib-induced effect of inhibition of LUAD cells. A, B. cMyc expression transfected with plasmids was evaluated by western blotting in A549 and PC-9 cells. C, D. After transfection with c-Myc vectors, cell viability under onvansertib exposure was then detected.



Supplementary Figure 2. The protein levels of Akt and p-Akt were evaluated by Western blot. A. Expression levels of Akt and p-Akt after the treatment of onvansertib in A549 cells. B. Expression levels of Akt and p-Akt after the treatment of onvansertib in PC-9 cells.